Roaming Dynamics in Formaldehyde-d_2 Dissociation†

Vasiliy Goncharov,‡ Sridhar A. Lahankar,‡,& John D. Farnum,§,# Joel M. Bowman,§ and Arthur G. Suits*,‡

Department of Chemistry, Wayne State University, Detroit, Michigan 48202, and Department of Chemistry and Cherry L. Emerson Center for Scientific Computation, Emory University, Atlanta, Georgia 30322

Received: July 2, 2009; Revised Manuscript Received: August 12, 2009

State-resolved photodissociation dynamics of formaldehyde-d_2, i.e., D_2CO, at energies slightly above the deuterium atom elimination channel have been studied both experimentally and theoretically. The results showed a clear bimodal distribution of energy into molecular photofragments. Substantial translational excitation of products at high rotational levels of CO was observed together with the D_2 cofragment in moderately excited vibrational levels, whereas rather small translational energy release of CO in low rotational levels was matched by a large degree of vibrational excitation in the D_2 molecule. An analogous distribution of energy in two distinct channels has been recently observed under similar conditions in H_2CO photolysis and attributed to two different dissociation pathways, namely, a pathway via the conventional transition state geometry and the previously unobserved pathway, deemed "roaming". Our experimental and theoretical data indicated that the same two dissociation pathways were responsible for the bimodal energy distribution into the molecular fragments resulting from the photolysis of D_2CO. Energy partitioning into molecular products was compared between photolysis of H_2CO and D_2CO at energies slightly above the H/D atom abstraction threshold.

I. Introduction

State-to-state dynamics of unimolecular decomposition of formaldehyde and its isotopologue D_2CO has been studied in great detail by the Moore group in Berkeley.[1−5] One of the most intriguing phenomena that eventually captured our interest in these molecular systems was the appearance of two distinct pathways of energy partitioning into the molecular photofragments[6] after excitation at or above the energy of the radical channel (1) and subsequent fast internal conversion (IC):

$$H_2CO \xrightarrow{h\nu} H_2CO(S_1) \xrightarrow{IC} H_2CO(S_0 \text{ or } T_1;v',J') \xrightarrow{ISC} H + HCO \quad (1)$$

$$H_2CO \xrightarrow{h\nu} H_2CO(S_1) \xrightarrow{IC} H_2CO(S_0;v',J') \rightarrow H_2(\text{low } v'') + CO(\text{high } J'') \quad (2)$$

$$H_2CO \xrightarrow{h\nu} H_2CO(S_1) \xrightarrow{IC} H_2CO(S_0;v',J') \rightarrow [H\cdots HCO] \rightarrow H_2(\text{high } v'') + CO(\text{low } J'') \quad (3)$$

The first molecular pathway is attributed to decomposition of formaldehyde to closed shell molecular products (2) on the ground state potential energy surface (PES) and is successfully explained by transition state theory (TST).[7] The geometry of the transition state (TS) complex dictates the energy partitioning into the molecular fragments leading to highly rotationally excited CO and low degrees of vibrational excitation in H_2. This pathway opens at the excitation energies near or above the TS barrier and, due to this rather high barrier, significant translational energy release is observed, characteristic of the dissociation of the closed shell precursor to the closed shell products.

Van Zee et al.[6] were the first to report that at the excitation energy roughly equal or above the opening of the radical channel (1) a small shoulder at very low rotational levels appeared in addition to the dominant highly excited CO rotational distribution originating from the "conventional" TST molecular channel (2). The authors ascribed the observed bimodal energy distribution into CO fragments to either anharmonicity of the TS at the energies near the opening of channel (1) or to the existence of a second fragmentation path (3) accessed through the channel (1). Recently, the Suits group[8−15] examined this interesting phenomenon using a DC-slice velocity map imaging approach and achieved sufficiently resolved velocity distributions of each quantum state of CO fragment to correlate it with fully resolved vibrational and a partially rotationally resolved structure of the H_2 cofragment. The resulting state-correlated data revealed that, in addition to drastically different rotational energy partitioning, bimodality in overall translational energy of the photofragments and, therefore, vibrational energy in the H_2 cofragment was always present once the excitation energy becomes comparable to or higher than the H atom elimination channel (1). This data, combined with the Bowman group's QCT calculations[8] served as very compelling evidence of the non-TST photodissociation pathway (3) of formaldehyde, where, in the course of hydrogen atom elimination, some H atoms stay in the vicinity of HCO fragment and "roam" on the flat ground state PES of formaldehyde until they find favorable geometry to abstract another

† Part of the "Vincenzo Aquilanti Festschrift".

* Corresponding author. E-mail: asuits@chem.wayne.edu.
‡ Wayne State University.
& Present address: Department of Chemistry, Montana State University, Bozeman, MT.
§ Emory University.
# Present address: Georgia Tech Research Institute, Atlanta, GA 30332.

10.1021/jp906248j CCC: $40.75

hydrogen atom from HCO. Because of the nature of the long-range interactions of the roaming H atom with HCO cofragment and the strongly exoergic H abstraction reaction, the resulting H_2 is highly vibrationally excited, and the energy partitioned into translational and rotational motions of the molecular fragments is rather small.

There are no a priori criteria limiting roaming events to relatively simple systems like formaldehyde or to the roaming of an H atom only. Indeed, recent velocity map-imaging studies of photodissociation dynamics in acetaldehyde[16] and acetone[17] also yielded bimodal distribution of molecular photofragments closely resembling the one observed in the roaming behavior of the formaldehyde system. In these cases it is the CH_3 radical that is speculated to participate in roaming events. However, the complexity of the studied molecules precludes the possibility of obtaining fully state-correlated data, so the evidence for roaming dynamics is not as compelling as for formaldehyde. Nevertheless, the latest experimental investigation of dissociation dynamics of acetaldehyde by Heazlewood et al.[18] revealed additional evidence supporting the roaming mechanism. Their FTIR emission spectra showed that the CH_4 photofragment was in highly vibrationally excited states, just like the H_2 cofragment resulting from roaming events in formaldehyde. Moreover, the theoretical efforts of Heazlewood et al.[18] indicated that roaming was a major pathway leading to molecular products in acetaldehyde.

In this combined experimental and theoretical study we present strong evidence of D atom roaming events occurring during the D_2CO photodissociation at the energies slightly above the opening of deuterium atom elimination channel.

II. Experimental Section

The DC slice[19] velocity map imaging technique was employed to acquire the translational energy distributions of rotational state resolved CO fragments resulting from the photolysis of formaldehyde-d_2. This approach permits one to record a narrow slice through the center of a three-dimensional ion cloud, directly yielding the product velocity distributions in real time.[20]

The velocity map imaging apparatus has been previously described in great detail.[11,19] Briefly, formaldehyde-d_2 was generated using the procedure reported by Terentis et al.,[21] seeded in 1 atm of Ar and the resulting gas mixture was introduced into the apparatus with a pulsed piezoelectric nozzle. In a source chamber the molecular beam underwent supersonic expansion into a velocity imaging chamber ensuing very low rotational temperatures on the order of 10 K. D_2CO was then photolyzed by a 319 nm laser beam generated by doubling the output of a dye laser (ScanMate, Lambda Physik) pumped by the second harmonic of an Nd:YAG laser (Spectra-Physics, DCR-3). The excitation wavelength was tuned to the $^rR_1(1)$ rotational level of the 2^24^3 vibrational band of the S_1 state of formaldehyde-d_2. Rapid internal conversion to the highly vibrationally excited ground state of formaldehyde-d_2 and subsequent dissociation leads to molecular fragments D_2 and CO. A 230 nm laser beam was introduced to resonantly ionize the CO photofragments via the Q-branch of the (2 + 1) REMPI $B\,^1\Sigma^+$ (v'=0) ← $X\,^1\Sigma^+$ (v''=0) transition. This wavelength was achieved by sum frequency mixing of the fundamental output of the third harmonic of seeded YAG laser (Spectra Physics, Quanta-Ray PRO 250) and a fundamental output of a dye laser (Sirah, PrecisionScan) pumped by the second harmonic of the same YAG laser. A stack of velocity focusing plates was used to send the resulting ions to an MCP detector with a phosphor screen. The velocity distribution images of CO ions were recorded with a standard video camera placed behind the phosphor screen. The images on- and off-resonance with the ionization laser were collected for the same amount of time under identical conditions to subtract a strong background signal of CO^+, dependent on both photolysis and ionization lasers and likely arising from the dissociative ionization of D_2CO. The background was resonant with the photolysis laser and present for all the transitions of D_2CO near the opening of the radical channel and was independent of the ionization laser wavelength. Introducing a delay of 300 ns between the photolysis and ionization lasers greatly reduced the nonresonant CO^+ contribution but also resulted in artificial anisotropy of the images as some ions traveling perpendicular to the laser propagation direction had enough time to leave the ionization volume.

III. Theoretical Section

To simulate the formaldehyde-d_2 fragmentation reaction, quasiclassical trajectory (QCT) calculations were done on the D_2CO potential energy surface. A sample of 10 000 trajectories was run at each set of total energy levels. The simulations were initiated in a configuration where all of the atoms are in equilibrium geometry except for one of the H−C bonds, which is stretched. This results in a system with 5 real normal modes and one imaginary normal mode. The motion of the atoms was initialized by adding zero point energy to each of the normal modes and then randomizing the phases. Then the remaining energy was added to the imaginary normal mode. A variety of methods for initializing the calculation have been previously investigated and the change in results was insignificant. So, we used this method to localize the energy in the CH vibration and shorten the calculation time.

The geometry of the molecule was analyzed at each time step, and if the configuration matched one of the predefined dissociation configurations, then the calculation was stopped and the position and velocity of each atom recorded. There was also an upper limit set on the number of time steps. If a calculation reached the limit without achieving any of the dissociation criteria, then the trajectory was thrown away. The upper limit was varied to ensure that the results were not being significantly altered by premature stopping times. After all of the simulations were run, the final states of the trajectories were analyzed. The internal energies of the diatomic fragments were calculated and if the total vibrational energy was below the zero-point energy of the fragment, then the trajectory was discarded. (Very few trajectories fall into this category.) The remaining trajectories were binned into quantum states by standard methods. Namely, the classical angular momentum of each diatom was determined and rounded to the nearest integer. Then the vibrational quantum number was assigned by comparing the total internal energy of the diatom to a table of exact ro-vibrational energies obtained by solving the ro-vibrational Schroedinger equation for the separated diatom and assigning the vibrational quantum to the closest ro-vibrational eigenvalue for the given rotational quantum number.

IV. Results and Discussion

DC sliced velocity map images of CO product in several degrees of rotational excitation: $J'' = 23$, 28, and 55 photofragmented from D_2CO are given in Figure 1. Corresponding internal energies of D_2 cofragment inferred from the velocity map images of CO along with calculated internal energies of D_2 using QCT are shown in Figure 2. In this plot, internal energy axis was chosen rather than a "conventional" translational energy axis to show that the rovibrational structure of D_2 was

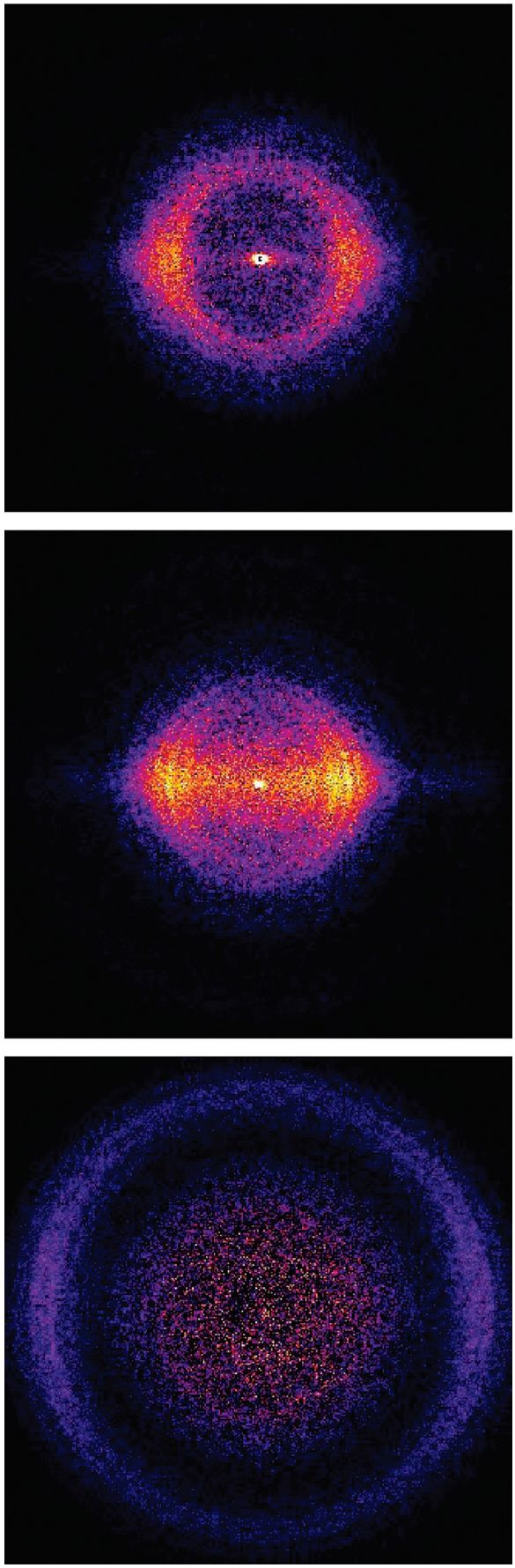

Figure 1. DC sliced velocity map images of CO fragments in several degrees of rotational excitation: $J'' = 23$, 28, and 55 from the 327 nm photolysis through the $^rR_1(1)$ rotational level of the 2^24^3 vibrational band of the S_1 state of D_2CO.

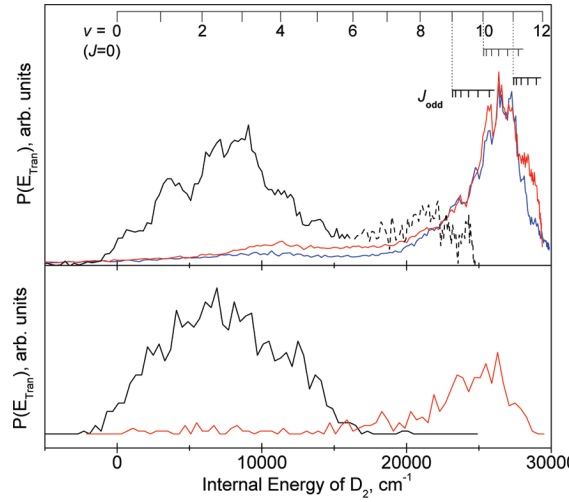

Figure 2. (Top) Internal energies of D_2 cofragment inferred from the velocity map images of CO in the rotational level $J'' = 23$ (blue line), 28 (red line), and 55 (black line). (Bottom) Internal energies of D_2 predicted using QCT calculations to correlate with CO in the rotational levels from $J'' = 21$ to 25 (red line) and from $J'' = 53$ to 57 (black line).

reproducible for $J'' = 23$ and 28 and to facilitate the comparison of the internal energies of D_2/H_2 products from the photodissociation of D_2CO and H_2CO. Figure 3 presents DC sliced velocity map images of CO product at $J''(CO) = 28$ and 45 produced through the 2^24^1 vibrational band of the S_1 state of H_2CO. Resulting internal energies of the H_2 cofragment are depicted in Figure 4. The photolysis wavelengths were carefully chosen to facilitate the comparison of the energy partitioning in the H_2CO and D_2CO systems. In the case of the D_2CO photolysis, the excess energy above the radical threshold of D_2CO[22] was $\sim$350 cm^{-1}, so the 2^24^1 vibrational band of H_2CO was chosen to match that excess energy. Figures 3 and 4 clearly show that the available energy in both D_2CO and H_2CO is partitioned into the photofragments in two distinct ways. The larger translational energy release products, correlated with D_2 in vibrational levels from 0 to 5, are associated with CO in highly excited rotational states and can be detected above as well as below the D atom elimination channel threshold. Energy distribution for this pathway is closely resembling the one observed for the H_2CO photolysis through the molecular channel pathway shown in Figure 4 and is successfully described by the TS theory.[7] At the excitation energies above the D atom elimination threshold much smaller translational energy release products, correlated with D_2 in vibrational levels from 9 to 11, are also detected for low degrees of rotational excitation of CO. The way the available energy partitioned into the D_2 and CO products above the D atom abstraction channel is analogous to the one in roaming mechanism for the H_2CO photodissociation. As expected, the peak of translational energy distribution obtained at the same degree of rotational excitation of CO from H_2CO and D_2CO for both pathways is shifted to higher vibrational quanta for D_2CO due to the fact that the vibrational frequency of H_2 is roughly 1.4 times larger than that of D_2. Nevertheless, as can be seen from Figures 2 and 4, the total internal energies of H_2 and D_2 fragments are roughly the same. This observation is in agreement with the Moore group[5,6] LIF studies of the D_2CO and H_2CO photolysis through the 2^14^1 and 2^24^3 vibrational bands. They also found that the average total internal energies of H_2 and D_2 are about the same. In addition, they detected a noticeable increase in the amount of rotational excitation of CO produced from D_2CO, which was fully

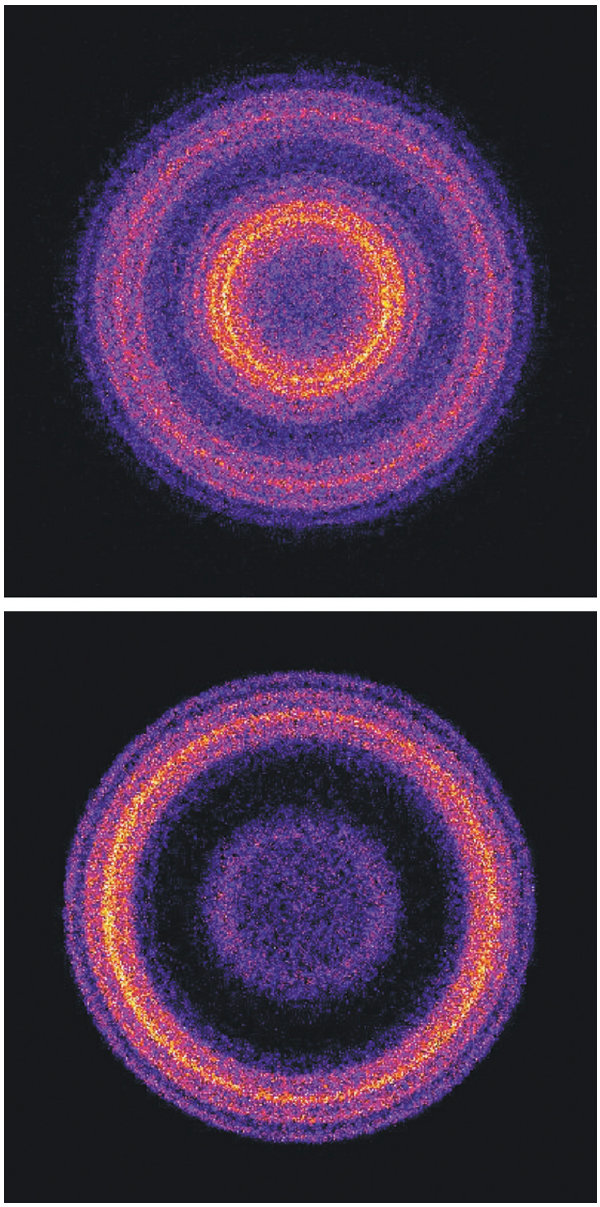

Figure 3. DC sliced velocity map images of CO fragments detected at $J''(CO) = 28$ and 45 from the 326 nm photolysis through the $2^2 4^1$ vibrational band of the S_1 state of H_2CO.

compensated by the decrease in the translational energy release. We also observed that the $J''(CO)$ peaks around 55 for D_2CO, whereas for H_2CO the maximum of $J''(CO)$ is around 40. This is in fair agreement with Schinke's predictions[23] using the rotational reflection principle to show that the shift of the maximum of $J''(CO)$ scales with the square root of the reduced mass when H_2 is substituted by D_2.

One important question in comparing H_2CO and D_2CO is the relative fraction of roaming events in these two systems. In the previous study on H_2CO, our group reported that 18% of the total molecular products were formed via roaming on the $2^1 4^3$ transition, just above the radical threshold.[12] This result was obtained by measuring the roaming yield on many individual rotational levels, then scaling the results by the rotational distribution given by van Zee et al. However, background interference in the D_2CO system has precluded similar measurements across many rotational levels in this system. Nevertheless, we can still estimate a lower bound for roaming events in D_2CO simply on the basis of our observation

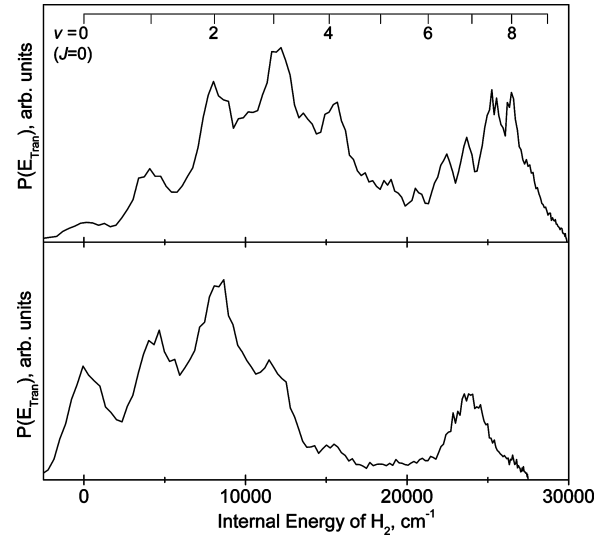

Figure 4. Internal energies of H_2 cofragment inferred from the velocity map images of CO detected at $J''(CO) = 28$ and 45.

that at $J''(CO) = 28$, all of the detected yield corresponds to roaming-type events. If we assume that all the events for $J''(CO) = 28$ and below are roaming, and all above 28 are not, we can simply integrate the van Zee rotational distributions (topmost plot of Figure 3 of ref 6) to get the roaming fraction. This estimate gives a minimum of 15% branching to roaming for D_2CO on the $2^2 4^3$ band. This is quite similar to the 18% seen for H_2CO at a comparable energy, and suggests that the increased mass does not inhibit roaming significantly.

V. Conclusion

The photolysis of formaldehyde-d_2 at the energies slightly above the D-atom elimination channel threshold results in bimodal energy distribution into the molecular fragments. DC sliced velocity map images along with quasi-classical trajectory simulations provide compelling evidence for the existence of a roaming pathway for the D_2CO photodissociation. The partitioning of energy into the photofragments is very similar for the photolysis of H_2CO and D_2CO. In particular, the internal energy of H_2 and D_2 fragments are roughly the same. However, there is a noticeable increase in the degree of the rotational excitation of CO produced from D_2CO, which is fully compensated by the decrease in the translational energy release.

Acknowledgment. This work was supported by the Director, Office of Science, Office of Basic Energy Science, Division of Chemical Science, Geoscience and Bioscience, of the US Department of Energy under contract number DE-FG02-04ER15593.

References and Notes

(1) Yeung, E. S.; Moore, C. B. *J. Chem. Phys.* **1974**, *60*, 2139.
(2) Houston, P. L.; Moore, C. B. *J. Chem. Phys.* **1976**, *65*, 757.
(3) Ho, P.; Bamford, D. J.; Buss, R. J.; Lee, Y. T.; Moore, C. B. *J. Chem. Phys.* **1982**, *76*, 3630.
(4) Moore, C. B.; Weisshaar, J. C. *Annu. Rev. Phys. Chem.* **1983**, *34*, 525.
(5) Bamford, D. J.; Filseth, S. V.; Foltz, M. F.; Hepburn, J. W.; Moore, C. B. *J. Chem. Phys.* **1985**, *82*, 3032.
(6) van Zee, R. D.; Foltz, M. F.; Moore, C. B. *J. Chem. Phys.* **1993**, *99*, 1664.
(7) Scuseria, G. E.; Schaefer, H. F., III. *J. Chem. Phys.* **1989**, *90*, 3629.
(8) Townsend, D.; Lahankar, S. A.; Lee, S. K.; Chambreau, S. D.; Suits, A. G.; Zhang, X.; Rheinecker, J.; Harding, L. B.; Bowman, J. M. *Science* **2004**, *306*, 1158.

(9) Chambreau, S. D.; Townsend, D.; Lahankar, S. A.; Lee, S. K.; Suits, A. G. *Phys. Scr.* **2006**, *73*, C89.
(10) Chambreau, S. D.; Lahankar, S. A.; Suits, A. G. *J. Chem. Phys.* **2006**, *125*, 044302.
(11) Lahankar, S. A.; Chambreau, S. D.; Townsend, D.; Suits, F.; Farnum, J.; Zhang, X.; Bowman, J. M.; Suits, A. G. *J. Chem. Phys.* **2006**, *125*, 044303.
(12) Lahankar, S. A.; Chambreau, S. D.; Zhang, X. B.; Bowman, J. M.; Suits, A. G. *J. Chem. Phys.* **2007**, 126.
(13) Suits, A. G.; Chambreau, S. D.; Lahankar, S. A. *Int. Rev. Phys. Chem.* **2007**, *26*, 585.
(14) Lahankar, S. A.; Goncharov, V.; Suits, F.; Farnum, J. D.; Bowman, J. M.; Suits, A. G. *Chem. Phys.* **2008**, *347*, 288.
(15) Suits, A. G. *Acc. Chem. Res.* **2008**, *41*, 873.
(16) Rubio-Lago, L.; Amaral, G. A.; Arregui, A.; Izquierdo, J. G.; Wang, F.; Zaouris, D.; Kitsopoulos, T. N.; Banares, L. *Phys. Chem. Chem. Phys.* **2007**, *9*, 6123.
(17) Goncharov, V.; Herath, N.; Suits, A. G. *J. Phys. Chem. A* **2008**, *112*, 9423.
(18) Heazlewood, B. R.; Jordan, M. J. T.; Kable, S. H.; Selby, T. M.; Osborn, D. L.; Shepler, B. C.; Braams, B. J.; Bowman, J. M. *Proc. Natl. Acad. Sci. U. S. A.* **2008**, *105*, 12719.
(19) Townsend, D.; Minitti, M. P.; Suits, A. G. *Rev. Sci. Instrum.* **2003**, *74*, 2530.
(20) Li, W.; Chambreau, S. D.; Lahankar, S. A.; Suits, A. G. *Rev. Sci. Instrum.* **2005**, *76*, 063106/1.
(21) Terentis, A. C.; Waugh, S. E.; Metha, G. F.; Kable, S. H. *J. Chem. Phys.* **1998**, *108*, 3187.
(22) Chuang, M. C.; Foltz, M. F.; Moore, C. B. *J. Chem. Phys.* **1987**, *87*, 3855.
(23) Schinke, R. *Annu. Rev. Phys. Chem.* **1988**, *39*, 39.

JP906248J